Frontiers in Environmental Research
ISSN: 2960-026X
DOI: 10.61784/fer3004

FLOOD SUSCEPTIBILITY MAPPING USING GIS – BASED MULTI – CRITERIA DECISION – MAKING "MCDM" METHOD: A CASE STUDY OF KANDAHAR PROVINCE, AFGHANISTAN

Ataullah Darzar*, Mohammad Karam Ikram
Engineering Faculty, Kandahar University, Kandahar, Afghanistan.
Corresponding Author: Ataullah Darzar, Email: ataullahdarzar@gmail.com

Abstract: Floods, which are common than other natural disasters like earthquakes, heavy precipitations, and droughts, are one the primary effects of global climate change and have major effects on human safety, sustainable development, and economic growth. As climate warming and intensifying hydrologic cycle worsen, global flooding risks may increase, potentially impacting Afghanistan as well. Severe flooding being caused by rising temperatures, erratic rainfall patterns, and extreme weather in Afghanistan, especially in the region of Kandahar. Despite the significance of identifying and mapping flood – prone areas, this province has not participated in any previous studies done on the topic at hand. Therefore, the aim of this research was to develop a flood susceptibility map for Kandahar province and identified flood – prone areas with high levels of occurrence by integrating Geographic Information System (GIS) and Multi – Criteria Decision – Making (MCDM) method, with Analytic Hierarchy Process (AHP). To achieve the study's goal, 11 Flood Causative Factors (FCFs), such as runoff potential, slope, rainfall, flow accumulation, distance from rivers, topographic wetness index (TWI), drainage density, lithology, Digital elevation model (DEM), sediment transport index (STI), and curvature, were weighted and overlayed. The resulting map depicted five different levels of susceptibility to flooding: least, low, moderate, high, and very high. The model's final map of flood susceptibility was found to be in line with past flood occurrences in the study area, demonstrating the successful outcome of the methodology utilized to locate and map flood – prone areas.
Keywords: Flood susceptibility map; GIS; MCDM; AHP; Kandahar Province; Afghanistan

1 INTRODUCTION

Relatively significant flows that surpass the natural pathways created for the runoff are referred to as floods. The river is at a high stage during a flood, and the river water typically overflows its banks [1]. Floods are serious natural calamities that have an impact on economic growth, sustainable development, and human safety, as a result of global climate change, floods are global problems that affect most of the world [2]. According to studies, floods have happened more frequently recently than other natural disasters, including earthquakes, heavy precipitations, and droughts [3]. In fact, the risk of worldwide flooding may rise in the future [4], due to warming climate and the resulting intensification of the hydrologic cycle [5]. For instance, studies indicate that even in most optimistic climate change scenario, sea levels are predicted to rise by 0.55 meters by 2100, endangering coastal cities, especially the larger one at risk [6]. Moreover, flood events are expected to occur more frequently in the southeast Asian region, east and central Africa, and a large portion of Latin America [7]. People in the world experience flood hazards every day. Many major floods have occurred worldwide in recent decades. For example, China in 1931 "which is thought to be the world's deadliest natural disaster and resulted in over 2 million deaths, is among the most deadly floods ever recorded" [8], floods in southeast Spain in 1997 [9], floods in south France in 2003 [10], flood events in the northwest Iberian Peninsula in 2000 [11], etc. Increased temperature, unpredictable rainfall patterns, and more extreme weather events are all causing higher level of severe flooding in Afghanistan. Such as, in 2019, with 97mm rain falling in 30 hours, Kandahar city and its surrounding districts experienced severe floods, and the event resulted in 20 fatalities and roughly 2000 homes being damaged [12]. Floods in Charikar, north of Kabul, in August 2020 killed over 100 people and collapsed hundreds of buildings [13]. Heavy flooding in the Spin Buldak district of Kandahar province, in August 2022 destroyed a large number of homes, farms, gardens, and other landscapes [14]. In April 2024, there were floods in 23 provinces of Afghanistan, then caused over 100 deaths and 54 injuries from heavy rains and flooding, at least 2134 houses were destroyed, 10789 animals perished, 800ha of farmland and 85Km of roads were damaged. The most affected areas were Kandahar, Herat, Western Farah, and Southern Zabul [15]. In July 2024, there were 40 fatalities, 25 injuries, and extensive infrastructure damage in several districts of the provinces of Badakhshan, Kunar, Laghman, Nangarhar, and Nuristan in eastern and northeastern Afghanistan due to strong windstorm, intense rains, and flash floods [16]. Furthermore, one of the afghan provinces that is particularly vulnerable to flooding during periods of high rainfall is Kandahar province. Therefore, the aim of the study was to create a flood susceptibility map for Kandahar province and identify flood – prone areas that are at high levels of flood occurrence. There are 3 types of methods for flood susceptibility mapping, 1st are Statistical methods, 2nd Soft computing methods, 3rd are MCDM methods [17]. Based on mathematical formulas, statistical methods are indirect ways to evaluate the connections between flood triggers and floods [18]. Soft computing is a numerical intelligence approach [19], that combine methods like Fuzzy Logic, Neural Networks (NNs), and Genetic Algorithms [20]. To improve results and solve specific problems [21], enhancing the analysis environment and decision

– making process and equating to human expertise [19]. A wide range of technical techniques for organizing decision issues and creating, assessing, and ranking potential decisions are offered by the Multi – Criteria Decision – Making (MCDM) methods [22]. This study used the Multi – Criteria Decision – Making MCDM method to identify flood – prone areas in Kandahar province, Afghanistan.

2 MATERIALS AND METHODS

2.1 Description of Study Area

This study is conducted on Kandahar province, which is one of the southern provinces of Afghanistan, sharing a border with Pakistan, to the south. It is surrounded by Helmand in the west, Uruzgan in the north and Zabul province in the east. The greater region surrounding the province is called LOY Kandahar. According to National Statistic and Information Authority (NSIA), the population of Kandahar province is approximately 1.5 million in 2021. The latitudinal extension of the province is from 29^o 31’ 32” N to 32^o 29’ 01” N, and the longitudinal extension of the province is from 64^o 26’ 46” E to 67^o 48’ 34” E. The province covers an area of 54022 km^2. location of the study area is shown below in Figure 1.

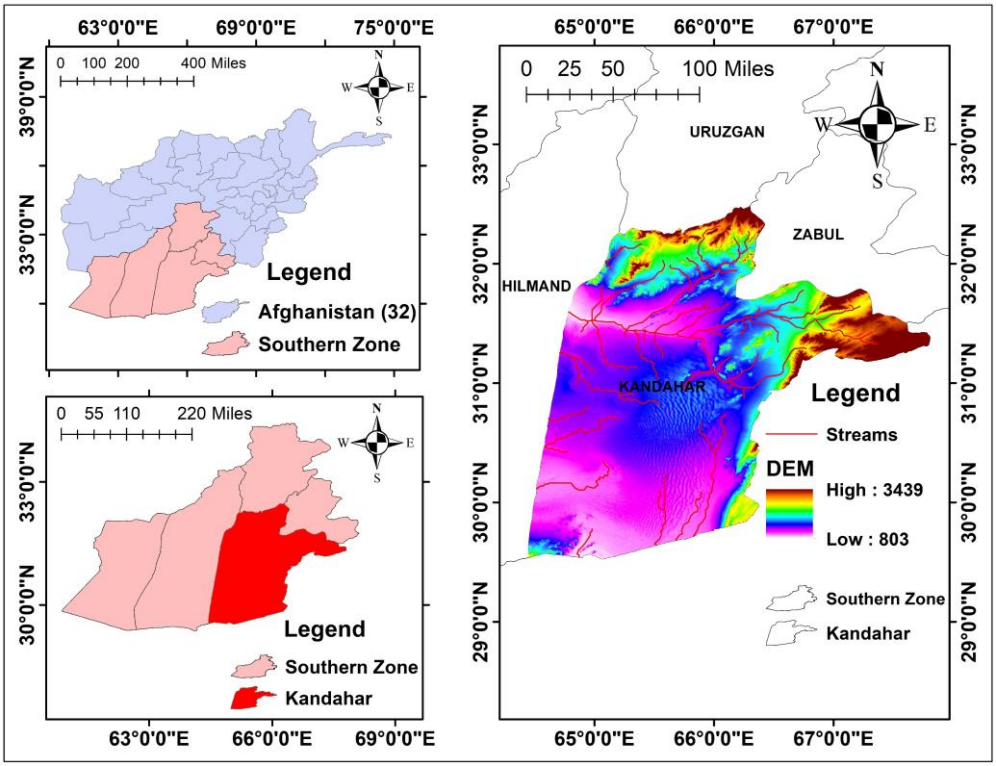

Figure 1 Study Area

2.2 Data and Sources

This study used open – access data (internet resources) to collect Remote Sensing (RS) data such as, land use/cover, soil, geology/lithology, rainfall, and Digital Elevation Model (DEM). Table 1 discusses all the sources from which the necessary data for this study was collected.

Table 1 Data and Sources

S. No	Data type	Original Format	Source
1	Soil	Vector	https://www.fao.org/soil-portal/data-hub/soil-mapsanddatabases/
2	Lithology	Vector	Afghan Geological Survey Department
3	Land use/cover	Raster	https://livingatlas.arcgis.com/landcover/
4	Rainfall	//	https://power.larc.nasa.gov/data-access-viewer/
5	DEM	Raster	USGS
6	River network	Vector	https://mapcruzin.com/free-Afghanistan-arcgis-mapsshapefiles.htm
7	Provincial boundary	Vector	https://mapcruzin.com/free-Afghanistan-arcgis-mapsshapefiles.htm

2.3 Methodological Flow Chart

The study area flood susceptibility map was developed by a process. The flood susceptibility map was created in four "4" stages utilizing the Geographic Information System GIS – based Multi – Criteria Decision – Making (MCDM) technique. The 1st stage involves the generation of all considered Flood Causative Factors (FCFs). The 2nd stage involves reclassifying all the considered FCFs. In 3rd stage, used the Analytic Hierarchy Process (AHP) to determine the weight of each FCF. The 4th stage is overlay analysis, which creates a flood susceptibility map. Figure 2 shows all 4 stages.

Figure 2 Flowchart of the Study

2.4 Generation of Flood Causative Factors "FCFs"

2.4.1 Digital elevation model (DEM)

Elevation is a factor considered when assessing flood danger. In general, Lower – Elevated regions are more likely to experience flooding than Higher – Elevated regions because they experience a greater proportion of river outflow and flood more quickly during high water flows [23].A 30m resolution Digital Elevation Model (DEM) of the Shuttle Radar Topography Mission (SRTM) is obtained for this study, and the study area DEM is then extracted using ARCGIS 10.7.1 platform. The DEM of the study area is shown in Figure 1(Study Area).

2.4.2 Flow accumulation

The flow direction is calculated to construct the flow accumulation throughout the runoff simulation procedure. The number of cells that flow through a certain cell determines the flow accumulation in that cell [24]. Greater flow accumulation values make a place more susceptible to flooding and simpler for runoff to form. To make flow accumulation map. Utilizing the DEM of the study area, the flow accumulation map is created. First, the flow direction map is created using the DEM, and then the flow accumulation map is created directly from the flow direction using Hydrology Tools in Arc toolbox. The flow accumulation map of the study area is shown below in Figure 3.

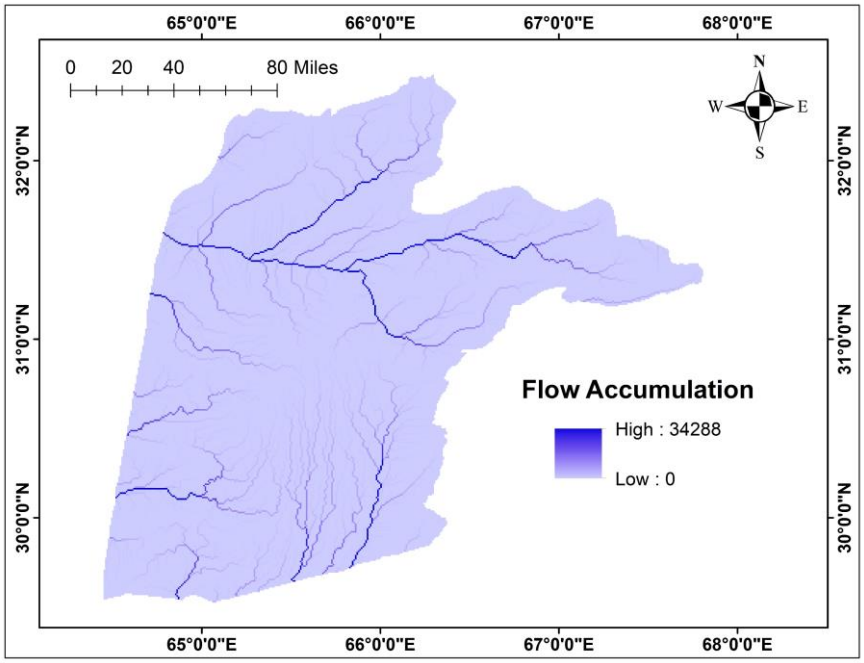

Figure 3 Flow Accumulation

2.4.3 Stream order and drainage density

Cells with accumulating flow above the threshold set by the user are referred to as stream orders. Many scholars have researched many methods for numerical definitions of stream orders; the most popular ones are the Shreve method [25], and Strahler method [26]. In each of these two methods, stream order is imagined as a tree with strong roots and slender branches in each of these two methods. However, these two approaches differ in how they identify the many branches at different levels. The stream that results from the merger of the rivers with different stream orders is assigned the higher of the two numbers [26]. The Shreve approach also assigns the outermost streams to the number 1 order. In contrast to the Strahler technique, which adds the two numbers at a connection [25]. The stream order is quantified in this study using the Strahler method, shown in Figure 4. Drainage density is defined as, the ratio of the total length of stream segments to total area of a drainage basin [27]. And calculated by the Equation 1. Flooding is more likely to occur in places with high drainage density than in areas with low drainage density. The drainage density map is created from stream order map using line density tool under density in spatial analyst tool. The study area's drainage density map is shown below in Figure 5.

$$D_d = \frac{\sum_{i=1}^{n} L}{A} \quad (1)$$

Where, D_d is the drainage density, n is the number of streams, L is the stream length (km), and A is the drainage basin (km).

2.4.4 Slope

The formation and dispersion of floods are significantly influenced by slope. The spread at which surface waterflows is determined by the land's slope. It is a signal that indicates how vulnerable the area is to flooding [28]. The amount of water covering the ground and the chance of a flood rise as the slope decreases and the velocity of surface waterflow decreases [29]. The higher slope found in mountainous areas regularly stop water from collecting and make the areas less susceptible to flooding [30]. The study area slope map is shown below in Figure 6.

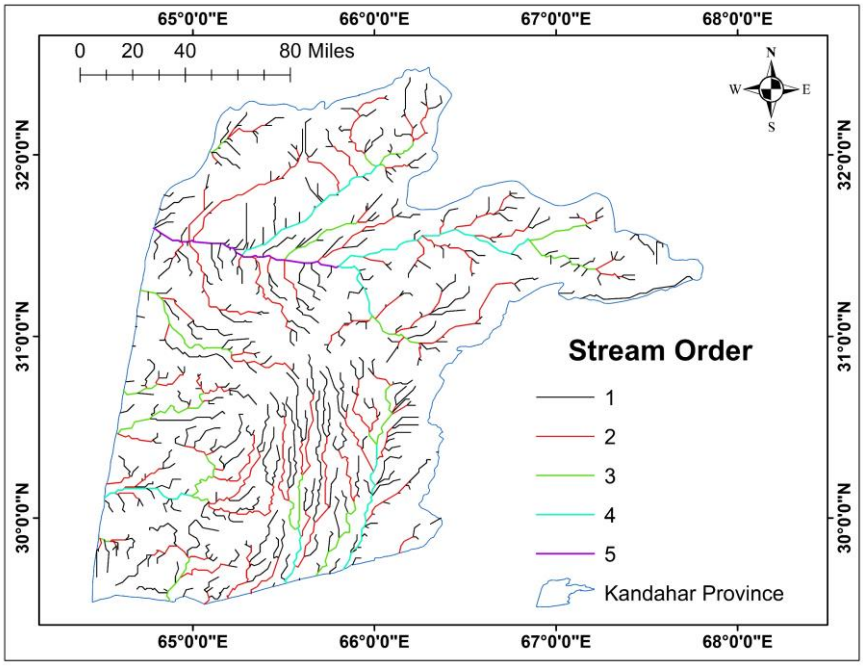

Figure 4 Stream Order (Strahler Classification)

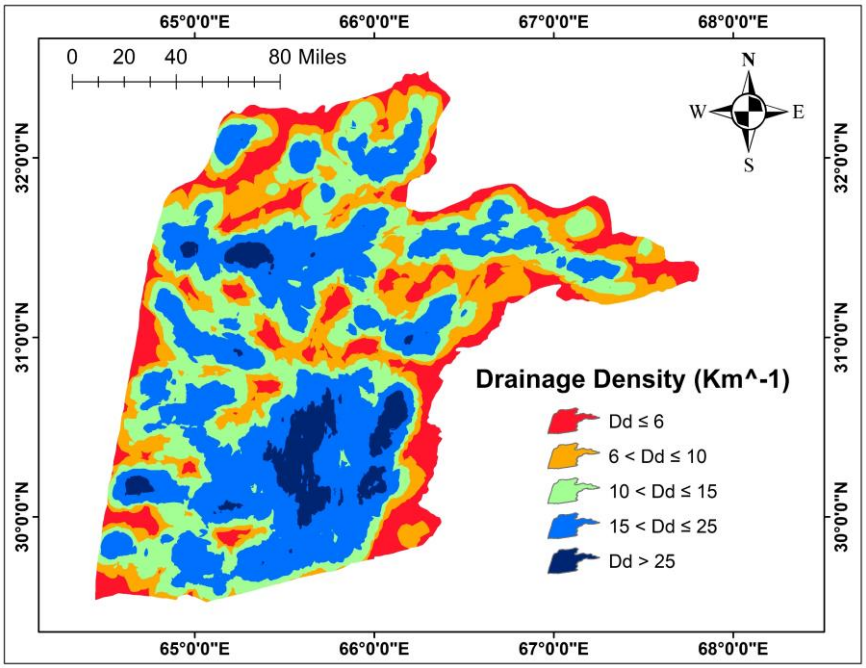

Figure 5 Drainage Density

2.4.5 Soil

Another factor that is frequently included in flood susceptibility mapping is soil type [17]. The type of soil has a major influence on the infiltration process [31]. The soil's fine texture composition increases surface runoff and decreases infiltration rate [31]. Therefor places with finer soil texture have a higher chance of flooding than areas with coarser soil texture [32]. The FAO/UNESCO soil map of the world is downloaded, and then the study area soil map is clipped from the world soil map using the geoprocessing tools in ARCGIS 10.7.1 platform, which is shown in Figure 7. Table 2 describes the 4 hydrological Soil Groups (HSGs) classification system based on runoff potential and infiltration rate, which is developed by the USDA – Soil Conservation Service [33]. Generally, there are 4 types of HSGs in the world, but the study area has two types, HSG – A and HSG – D. the brief explanation of the study area soil is discussed below in Table 3, and the study area HSG soil map is shown in Figure 8a.

2.4.6 Land use and land cover (LULC)

Land use and land cover are two of the most significant elements influencing the likelihood of floods. Despite their frequent interchange in literature, the terms "Land cover" and "Land use" are distinct. Land cover describes the physical and biological characteristics of the basin, such as its forests, arid regions, and wetlands, etc. that make up the nature of the basin. On the other hand, land use describes how the basin is used, including for farming, manufacturing, and settlements, and it is influenced by socioeconomic activities. Area with high densities of vegetation are frequently less

susceptible to flooding, because vegetation causes significant infiltrations and slow down the rapid flow of water [31]. Areas such as permanent wetlands, built up regions, settlements, barren land (Excluding Sand Dunes and Sand Cover), etc. are more susceptible to flooding. The study area landcover map is shown in Figure 8b.

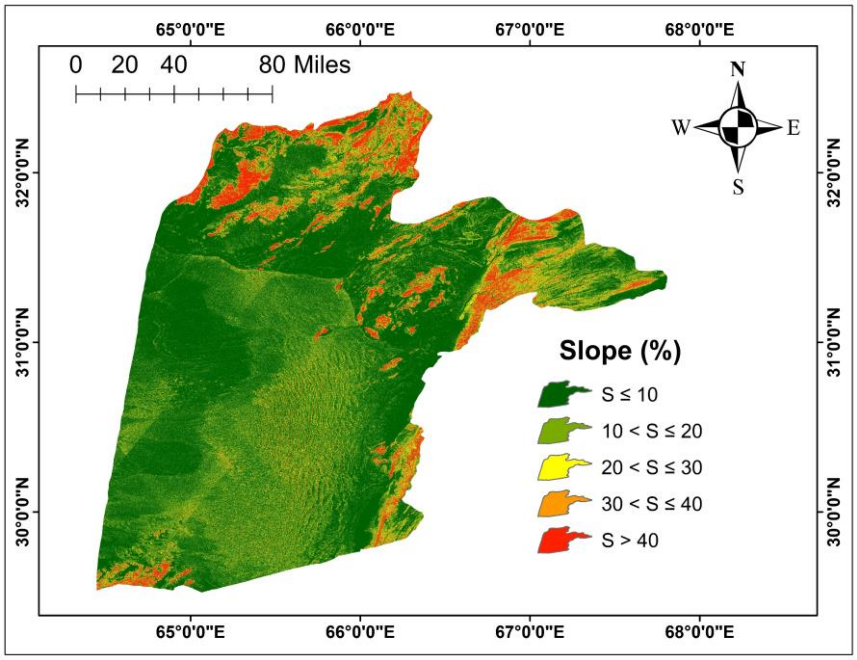

Figure 6 Slope Map of the Study Area

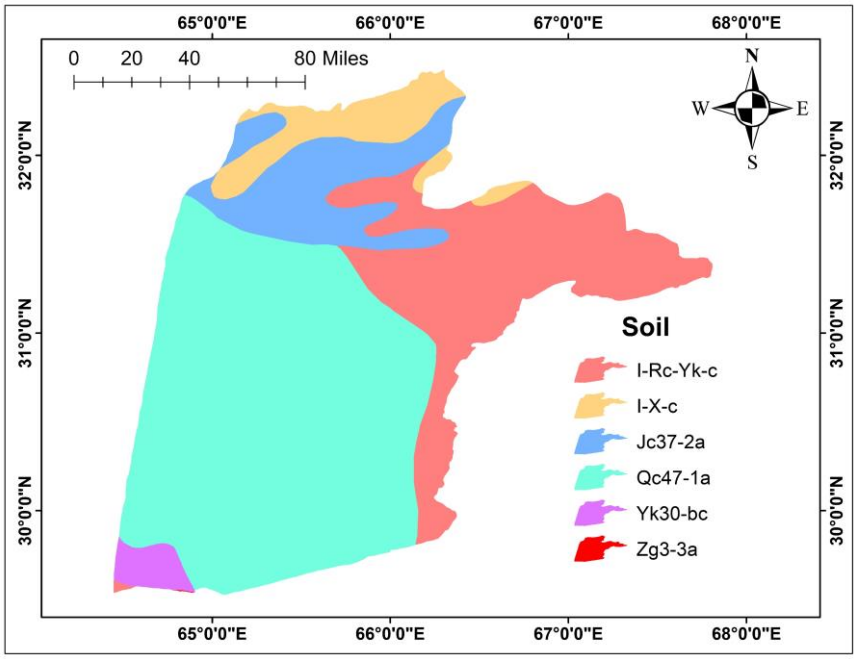

Figure 7 Soil Map of the Study Area

Table 2 Description of 4 HSGs

HSGs	Textures	Properties
A	Sand, loamy sand, or sandy loam	High infiltration rate, Low runoff potential
B	Silt loam or loam	Moderate infiltration rate, Moderately low runoff potential
C	Sandy clay loam	Low infiltration rate, Moderately high runoff potential
D	Clay loam, silty clay loam, sandy clay, silty clay, or clay	Very low infiltration rate, High runoff potential

Table 3 Description of Study Area Soils

SNUM	Map Symbol	FAO – Soil	Textural property			Texture	HSGs
			Sand (%)	Clay (%)	Silt (%)		
3508	I–Rc–Yk–c	Lithosols	35	26	39	Loam	D
3512	I–X–C	Lithosols	45	22	33	Loam	D
3525	Jc37–2a	Calcaric Fluvisols	47	18	35	Loam	D
3542	Qc47–1a	Cambic Arenosols	62	16	22	Sandy–Loam	A
3598	Yk30–bc	Calcic Yermosols	36	27	37	Loam	D
3621	Zg3–3a	Glayic Solonchaks	29	52	19	Clay	D

2.4.7 Curve number (CN)

The CN, a dimensionless number that depends on the Hydrologic Soil Groups (HSGs) and land cover of the particular area, ranges from 30 for permeable soils that has high rate of infiltration to 100 for waterbodies, snow, and ice [34]. Areas with higher number of CN are more vulnerable to flooding than areas with lower numbers of CN. The study area CN map is shown below in Figure 8c.

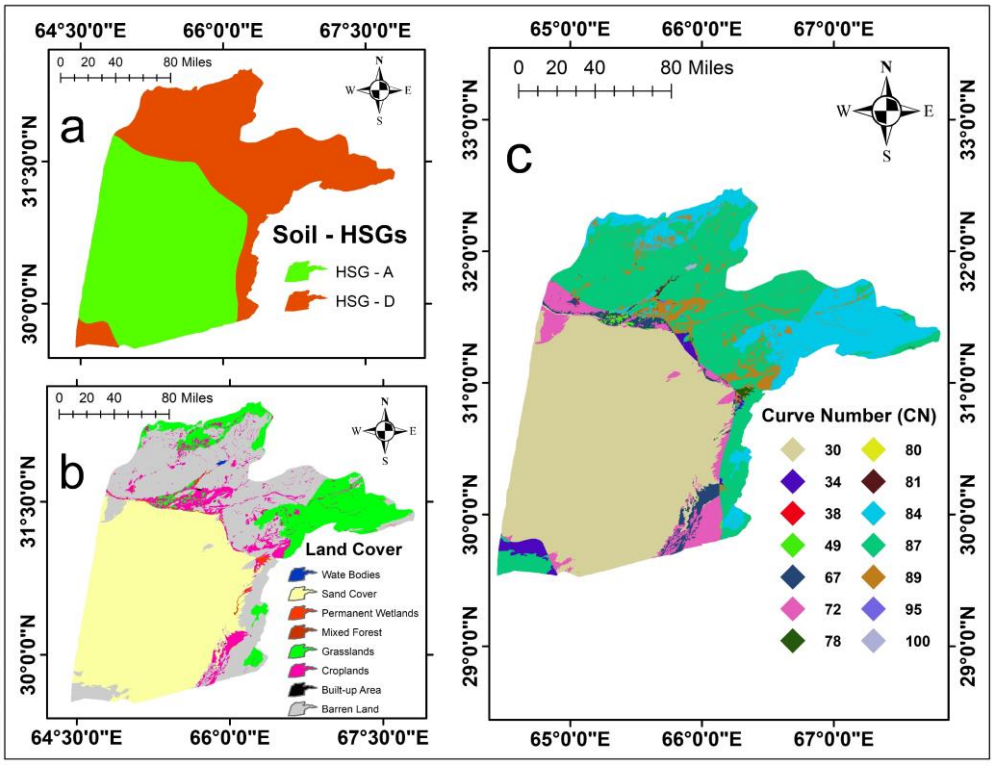

Figure 8 a, Soil HSGs. **b,** Land Cover. **c,** Curve Number

2.4.8 Rainfall

Rainfall is the most significant parameter that determine the likelihood of floods [35]. Rainfall needs to be taken into account in any estimate of flood susceptibility since without it, floods are unthinkable [31]. The spread of the flood, it's duration, it's range of influence, and potential damages to the area are all influenced by intensity, duration, and amount of the precipitation [17]. The study area rainfall data of 23 years "from 2000 to 2022" is downloaded from NASA power access site, then based on that data the rainfall map is created. Which is shown in Figure 9.

2.4.9 Runoff potential

Soil runoff potential is defined as the chances of surface runoff happening during rain falling and snow melting. When water moves through soil at a slow enough rate for water to flow across the surface of the land into waterbodies, this is known as surface runoff [36]. Higher runoff potential areas are typically more susceptible to flooding than lower runoff potential areas. To create the runoff potential map for the study area, use the Equation 2 through the "Map Algebra" tool in ARCGIS 10.7.1 platform.

$$Q = \frac{(P - I_a)^2}{P - I_a - S} \quad (2)$$

Where Q is runoff potential (mm), P is rainfall (mm), $I_a = 0.2S$ is initial abstraction, and S is potential maximum retention (mm) which is calculated using Equation 3. the study area runoff potential map is shown below in Figure 10.

$$S = \frac{25400}{CN} - 254 \quad (3)$$

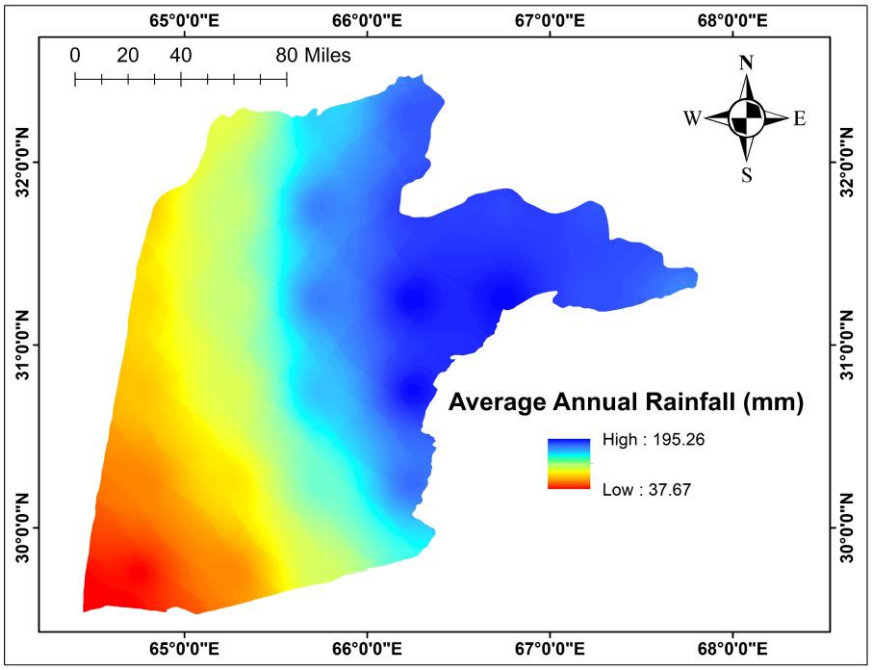

Figure 9 Rainfall Map of the Study Area

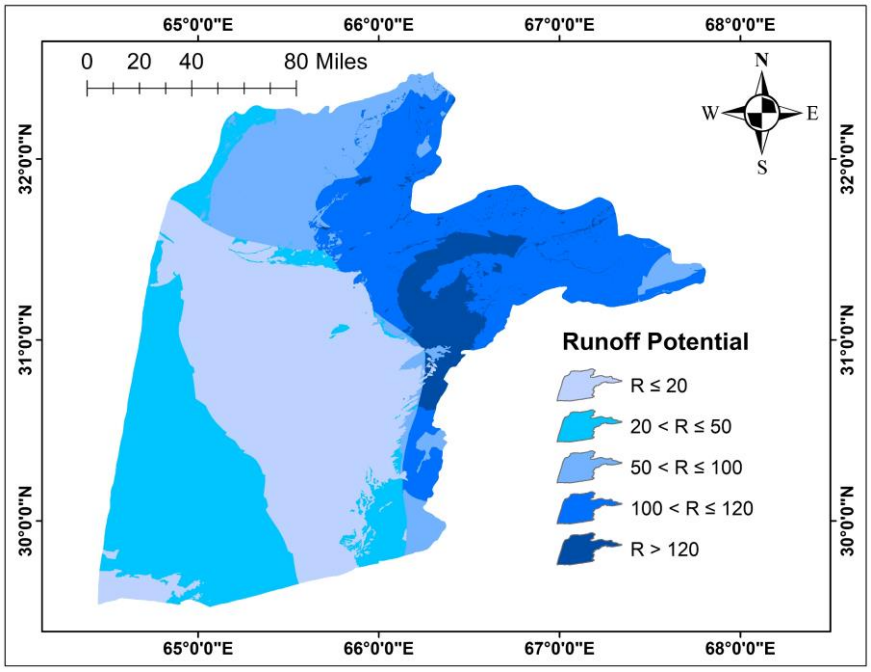

Figure 10 Runoff Potential Map of the Study Area

2.4.10 Topographic wetness index "TWI"

TWI is a key idea in the field of hydrology and geomorphology. It is used to evaluate and model the spatial distribution of potential wetness and water accumulation on a surface. It is a useful tool for land use planning, environmental management, and the conservation of natural resources since it helps to comprehend how water moves over different surfaces. The topographical influence on runoff generation and flow accumulation volume at a specific region is measured using TWI [31]. It describes the propensity of water under the influence of gravity to gather at a certain location or flow downward [37]. Flood danger is directly correlated with TWI; the higher the TWI score indicates a higher chance of flooding [38]. The TWI is calculated using Equation 4.

$$TWI = \ln\left(\frac{A_s}{\tan(\beta)}\right) \quad (4)$$

Where β indicates the slope gradient (in degrees) and A_s indicates catchment area. The TWI map of the study region is shown in Figure 11.

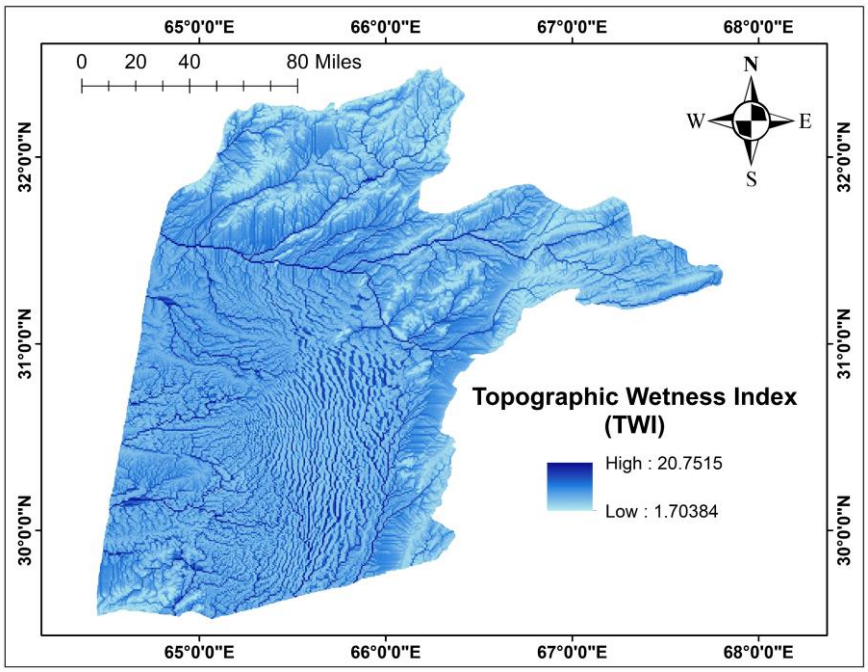

Figure 11 Topographic Wetness Index (TWI) of Study Area

2.4.11 Sediment transport index "STI"

STI has a strong connection with any region's runoff features. Flood events are more likely to occur in areas with low STI values, and vice versa [39]. The Equation 5 is used to get STI from DEM [40].

$$STI = \left(\frac{A_s}{22.13}\right)^{0.6} \times \left(\frac{Sin\beta}{0.0896}\right)^{1.3} \quad (5)$$

Where β indicates the slope gradient (in degrees) and A_s indicates catchment area. The STI map of the study region is shown in Figure 12.

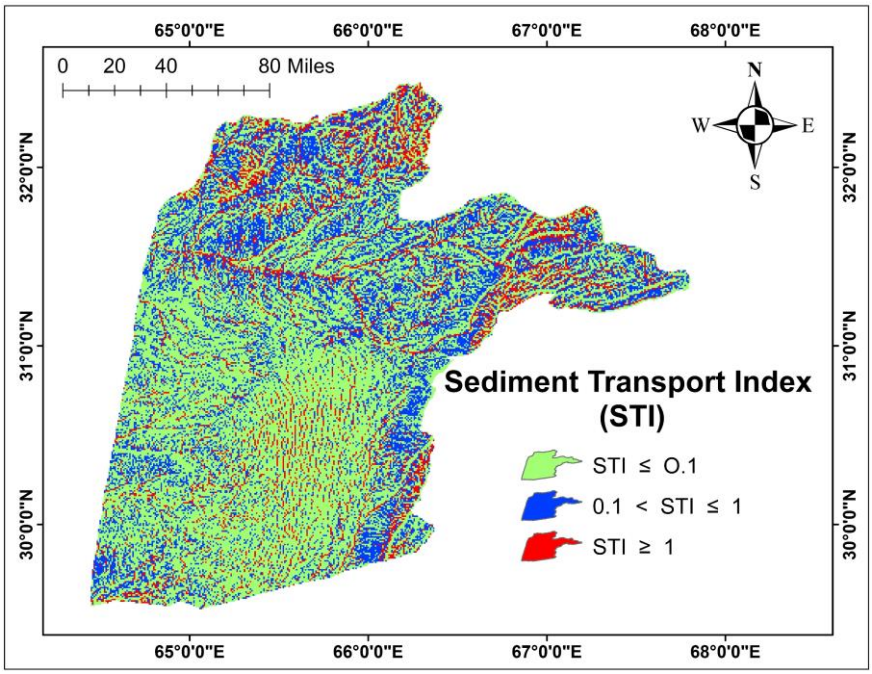

Figure 12 Sediment Transport Index (STI) of Study Area

2.4.12 Distance from river

The distance between a site and the river network affects, how far the flood spreads throughout the basin [41]. Due to the fact that excess water from rivers first reaches adjacent lowland areas and the side river banks, places near to rivers are more likely to experience flooding than areas farther from rivers [42]. The river network map of all country is downloaded, then the study area distance from river map is created through Euclidian distance tool under distance in spatial analyst tools in ARCGIS10.7.1 platform. The study area distance from rivers map is shown in Figure 13.

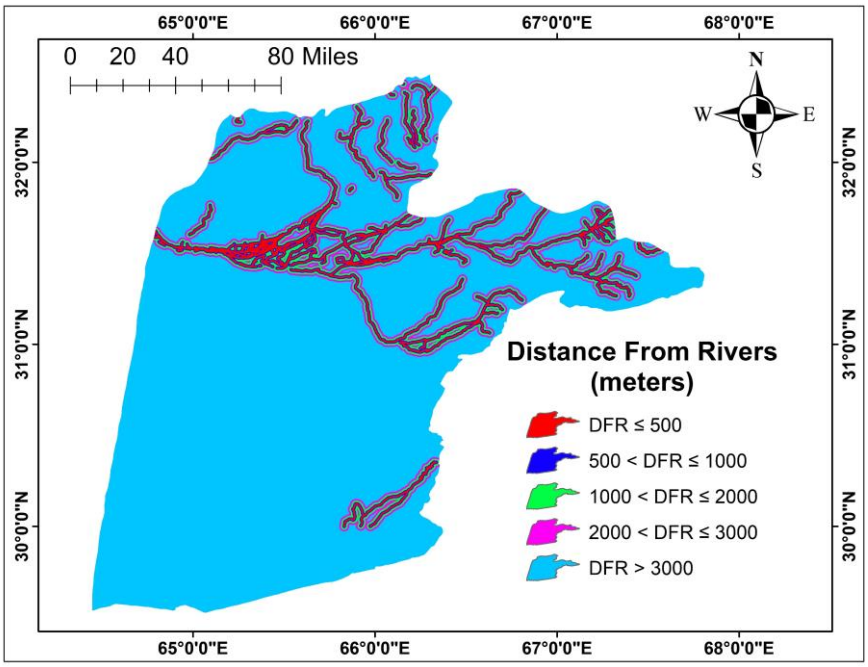

Figure 13 Distance from Rivers Map of Study Area

2.4.13 Geology/Lithology

Studies have demonstrated that formations with geologically impermeable surfaces are more vulnerable to flooding [43]. Simultaneously, geology plays a major role in the drainage pattern development process, which is linked to water accumulation processes and factors influencing the overflow capacity [44]. The lithology map of Afghanistan is obtained from "Afghan Geological Survey Department", then the study area lithology map is clipped from the gathered lithology map, which is shown in Figure 14. Then the study area lithology map is reclassified according to permeability which is shown below in Figure 15.

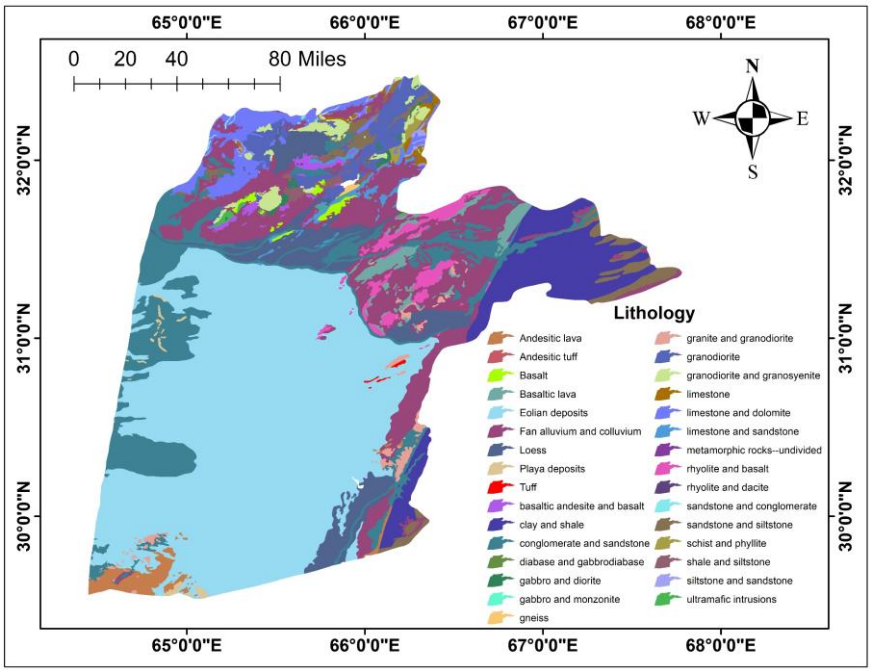

Figure 14 Lithology Map

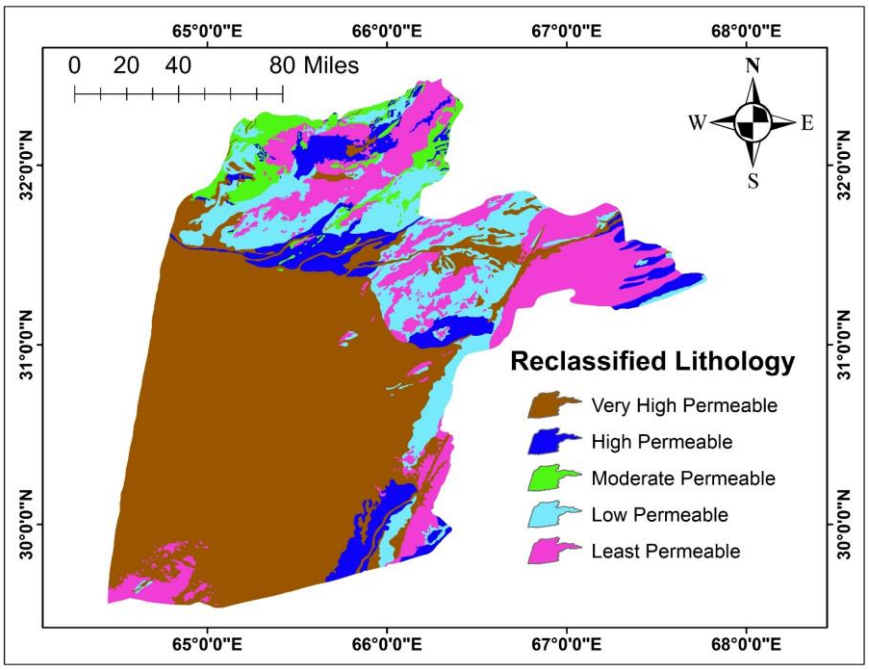

Figure 15 Reclassified Lithology Map

2.4.14 Curvature

This parameter represents processes connected to erosion, flow velocity, and accumulation [45]. Both flow and possibility of floods are impacted by curvature [46]. Floods also tend to happen in places where the curvature is flat [47, 48]. According to some studies the most accurate predictors of flood occurrences are elevation and curvature [49]. The study area curvature map is shown below in Figure 16.

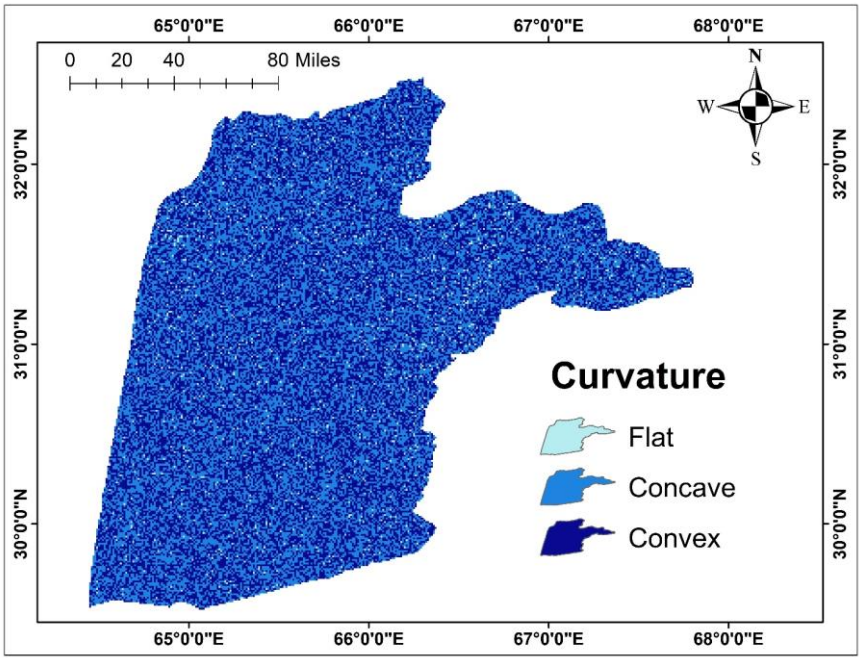

Figure 16 Curvature Map of the Study Area

2.5 Multi – Criteria Decision – Making "MCDM"

Selecting from a range of options is a part of the process of decision – making. MCDM is a procedure that allows values to be assigned to alternatives and several criteria to be evaluated simultaneously in complicated problems like disasters, and MCDM method, are those that enable the best option to be chosen from multiple criteria applied simultaneously [22]. Put another way, it is a technique that enables decision – makers to consider the effectiveness of numerous independent variables while reaching the best conclusion possible given the situation and relevant elements [50].

2.6 Reclassification of the Flood – Causative Factors (FCFs)

The 11 flood – causative factors were all reclassified based on their vulnerability to flooding using ArcGIS's reclassification tool, with using a 1 – 5 scale, where 1 denotes the least susceptibility to flooding, and 5 denotes the very high susceptibility to flooding, raster layers are reclassified into 5 classes. The only criteria that are reclassified into their respective 3 classes are Sediment transport index (STI) and curvature, each of which has three variants. Reclassification of the selected raster layers is described in Table 4.

Table 4 Reclassification of flood causative factors

Flood Causative factors	Classes	Flood Susceptibility	Ratings	Average Weight (%)
Runoff Potential (mm)	R ≤ 20	Least	1	24
	20 < R ≤ 50	Low	2	
	50 < R ≤ 100	Moderate	3	
	100 < R ≤ 120	High	4	
	R > 120	Very High	5	
Slope (%)	S ≤ 10	Very High	5	16
	10 < S ≤ 20	High	4	
	20 < S ≤ 30	Moderate	3	
	30 < S ≤ 40	Low	2	
	S > 40	Least	1	
Rainfall (mm)	Rf ≤ 60	Least	1	16
	60 < Rf ≤ 80	Low	2	
	80 < Rf ≤ 100	Moderate	3	
	100 < Rf ≤ 150	High	4	
	Rf > 150	Very High	5	
Flow Accumulation	Fa ≤ 500	Least	1	11
	500 < Fa ≤ 2000	Low	2	
	2000 < Fa ≤ 5000	Moderate	3	
	5000 < Fa ≤ 15000	High	4	
	Fa > 15000	Very High	5	
Distance from rivers (m)	D ≤ 500	Very High	5	11
	500 < D ≤ 1000	High	4	
	1000 < D ≤ 2000	Moderate	3	
	2000 < D ≤ 3000	Low	2	
	D > 3000	Least	1	
TWI	T ≤ 5	Least	1	7
	5 < T ≤ 9	Low	2	
	9 < T ≤ 13	Moderate	3	
	13 < T ≤ 16	High	4	
	T > 16	Very High	5	
Drainage Density	Dd ≤ 6	Least	1	5
	6 < Dd ≤ 10	Low	2	
	10 < Dd ≤ 15	Moderate	3	
	15 Dd ≤ 25	High	4	
	Dd > 25	Very High	5	
Lithology	Very high permeable	Least	1	4
	High permeable	Low	2	
	Moderate permeable	Moderate	3	
	Low permeable	High	4	
	Least permeable	Very High	5	
DEM (m)	803 – 1200	Very High	5	3
	1200 – 1500	High	4	
	1500 – 1900	Moderate	3	
	1900 – 2400	Low	2	
	2400 – 3439	Least	1	
STI	St ≤ 0.1	Very High	5	2
	0.1 < St ≤ 1	Moderate	3	
	St > 1	Least	1	
Curvature	Flat	Very High	5	1

Concave	Moderate	3
Convex	Least	1

2.7 Analytic Hierarchy Process (AHP)

Table 5, lists several main MCDM methods, with AHP being the most widely used. The AHP method, created by Thomas L. Saaty [51], is a more straightforward and effective approach for making decisions on complicated issues with multiple criteria. Since the early 21st century it has been widely used with GIS [52], providing a user – friendly solution by combining sophisticated tools for huge – data computing, visualization, and mapping with decision – making support approaches [53]. In this study, the AHP technique is carried out through the following 3 steps.

1st Step, create pairwise comparison decimal matrix Table 7: where weights were assigned to each factor to express the importance of each factor relative to other factors. This was done utilizing related review literature and professional opinion to fill a pairwise comparison decimal matrix. The Flood Causative Factors (FCFs) are graded on a scale of 1 to 9, with 1 stating equal significance and 9 stating one factor is extremely more significant than other. Saaty's pairwise comparison scale [54] is discussed below in Table 6.

2nd Step, calculated normalized pairwise matrix Table 8: after summing up all of the numbers in each column of the pairwise comparison decimal matrix Table 7, divide each column's entry by its column – wise sum to obtain the matrix's normalized score. The sum of each column in normalized pairwise matrix Table 8 should be 1. And the weight of each factor is calculated from a normalized pairwise matrix using the arithmetic mean of each factor's row in the normalized pairwise matrix.

3rd Step, Consistency ratio (CR): calculate the consistency ratio in order to assess the judgement's validity. And use CR < 0.1 "Acceptable" to verify the value. The CR value is calculated using Equation 6.

$$CR = \frac{CI}{RI} \tag{6}$$

Where: RI is the random inconsistency index and CI is the consistency index. Table 9, discusses the value of RI for the number of criteria (n), while Equation 7, is used to calculate CI.

$$CI = \frac{\lambda_{max} - n}{n - 1} \tag{7}$$

Where: n is the number of flood causative factors in AHP analysis, and λ_{max} is the total of the products of the column wise sum in pairwise comparison decimal matrix Table 10, and the average weights from normalized pairwise matrix.

Table 5 Main MCDM Techniques

Name	Full Name	Primary Author	Time
VIKOR	Vesekriterijunska Optimizacija I Kopromisno Resenje	Opricovic S.	1998
ANP	Analytic Network Process	Saaty T.L.	1996
PROMETHEE	Preference Ranking Organization method for Enrichment Evaluation	Brans J.P.	1984
TOPSIS	Technique for Order Preference by Similarity to an Ideal Solution	Hawang C.	1981
DEMATEL	Decision Making Trial and Evaluation Laboratory	Gabus A.	1972
AHP	Analytic Hierarchy Process	Saaty T.L.	1970
ELECTRE	Elimination and Choice Translating Reality	Benayoun R.	1966

Table 6 Saaty's Pairwise Comparison Scales

Numerical Values	Intensity of Importance
1	Activity is equally Important to another
3	Activity is moderately important to another
5	Activity is strongly important to another
7	Activity is very strongly important to another
9	Activity is extremely important to another
2,4,6,8	Intermediate values between the two adjacent judgments
Reciprocals	Values for inversion comparison of importance

Table 7 Pairwise Comparison Decimal Matrix

FCF	R	S	Rf	Fa	DFR	TWI	Dd	Litho	DEM	STI	Cu
R	1	2	2	3	3	4	5	6	7	8	9
S	0.5	1	1	2	2	3	4	5	6	7	8
Rf	0.5	1	1	2	2	3	4	5	6	7	8
Fa	0.333	0.5	0.5	1	1	2	3	4	5	6	7
DFR	0.333	0.5	0.5	1	1	2	3	4	5	6	7
TWI	0.25	0.333	0.333	0.5	0.5	1	2	3	4	5	6
Dd	0.2	0.25	0.25	0.333	0.333	0.5	1	2	3	4	5
Litho	0.167	0.2	0.2	0.25	0.25	0.333	0.5	1	2	3	4

DEM	0.143	0.167	0.167	0.2	0.2	0.25	0.333	0.5	1	2	3
STI	0.125	0.143	0.143	0.167	0.167	0.2	0.25	0.333	0.5	1	2
Cu	0.111	0.125	0.125	0.143	0.143	0.167	0.2	0.25	0.333	0.5	1
SUM	3.662	6.218	6.218	10.593	10.593	16.45	23.283	31.08	39.833	49.5	60

Where: R=Runoff potential, S=Slope, Rf=Rainfall, Fa=Flow accumulation, DFR=Distance from rivers, TWI=Topoghraphic wetness index, Dd=Drainage density, litho=Lithology, DEM=Digital elevation model, STI=Sediment transport index, Cu=Curvature

Table 8 Normalized Pairwise Comparison Matrix

FCF	R	S	Rf	Fa	DFR	TWI	Dd	Litho	DEM	STI	Cu	Weight
R	0.273	0.322	0.322	0.283	0.283	0.243	0.215	0.193	0.176	0.162	0.15	0.238
S	0.137	0.161	0.161	0.189	0.189	0.182	0.172	0.161	0.151	0.141	0.1333	0.161
Rf	0.137	0.161	0.161	0.189	0.189	0.182	0.172	0.161	0.151	0.141	0.1333	0.161
Fa	0.091	0.08	0.08	0.094	0.094	0.122	0.129	0.129	0.126	0.121	0.1167	0.108
DFR	0.091	0.08	0.08	0.094	0.094	0.122	0.129	0.129	0.126	0.121	0.1167	0.108
TWI	0.068	0.054	0.054	0.047	0.047	0.061	0.086	0.097	0.1	0.101	0.1	0.074
Dd	0.055	0.04	0.04	0.031	0.031	0.03	0.043	0.064	0.075	0.081	0.0833	0.052
Litho	0.046	0.032	0.032	0.024	0.024	0.02	0.021	0.032	0.05	0.061	0.0667	0.037
DEM	0.039	0.027	0.027	0.019	0.019	0.015	0.014	0.016	0.025	0.04	0.05	0.027
STI	0.034	0.023	0.023	0.016	0.016	0.012	0.011	0.011	0.013	0.02	0.0333	0.019
Cu	0.03	0.02	0.02	0.013	0.013	0.01	0.009	0.008	0.008	0.01	0.0167	0.014
SUM	1	1	1	1	1	1	1	1	1	1	1	1

Table 9 Random Inconsistency Index

n	1	2	3	4	5	6	7	8	9	10	11	12	13	14	15
RI	0	0	0.58	0.9	1.12	1.24	1.32	1.41	1.45	1.49	1.51	1.48	1.56	1.57	1.58

Table 10 Calculation of λ_{max}

Flood Causative Factors (FCFs)	Colum wise sum of FCFs	Average Weight	Product of both columns
Runoff Potential	3.662	0.238	0.873
Slope	6.218	0.161	1.004
Rainfall	6.218	0.161	1.004
Flow Accumulation	10.59	0.108	1.139
Distance from Rivers	10.59	0.108	1.139
Topographic Wetness Index	16.45	0.074	1.218
Drainage Density	23.28	0.052	1.217
Lithology	31.08	0.037	1.154
Digital Elevation Model	39.83	0.027	1.056
Sediment Transport Index	49.5	0.019	0.951
Curvature	60	0.014	0.87
		$\lambda_{max} = sum\ of\ the\ above \longrightarrow$	11.63

$$CI = \frac{\lambda_{max} - n}{n - 1} = \frac{11.63 - 11}{11 - 1} = 0.063$$

$$CR = \frac{CI}{RI} = \frac{0.063}{1.51} = 0.0417 < 0.1\ "Acceptable"$$

2.8 Overlay Analysis

In this study, the flood susceptibility map was created using overlay analysis under spatial analyst tools using the weighted overlay of the ARCGIS 10.7.1 platform. The tool assigns "Weight values multiplied by 100" and "Rating values" to the "Influence values" and "Scale values", respectively. Following the process of resampling every raster layer to an identical spatial resolution, weighted overlay analysis was performed. Where runoff potential is assigned with highest weight equal to 24, and curvature assigned with least weight equal to 1.

3 RESULTS AND DISCUSSIONS

The final flood susceptibility map of Kandahar province was created by combining 11 flood – causative factors thematic maps, and it was then divided into five classes: least, low, moderate, high, and very high, as shown in Figure 17. The research area's flood susceptibility map shows the vulnerability to flood levels as a percentage, with 33.894% being least to low, 53.051% being moderate, and 13.055% being high to very high. Figure 18 displays the area (Km^2) of flood susceptibility levels. The susceptibility map shows that the majority of the province falls within the range of least to moderate susceptibility, with the central, north, northeast, and southeast regions of the province representing the high to very high susceptible region. According to flood susceptibility map, the areas of Kandahar city and its surroundings, and districts including, Maruf, Daman, Arghistan, Arghandab, Spin Boldak, and Shah Wali Kot are most susceptible to floods. Table 11, discusses the area (%) and (Km^2) of all districts of the province, shows that the flood susceptibility classes, which used to be 5, have now dropped to 3, including least to low, moderate, and high to very high, for simplicity of understanding. The resulted flood susceptibility map was compared to historical flood event locations to ensure accuracy. The results indicate that the study's output is more accurate, with the majority of the locations falling within the high to very high flood susceptibility classes depicted in Figure 19.

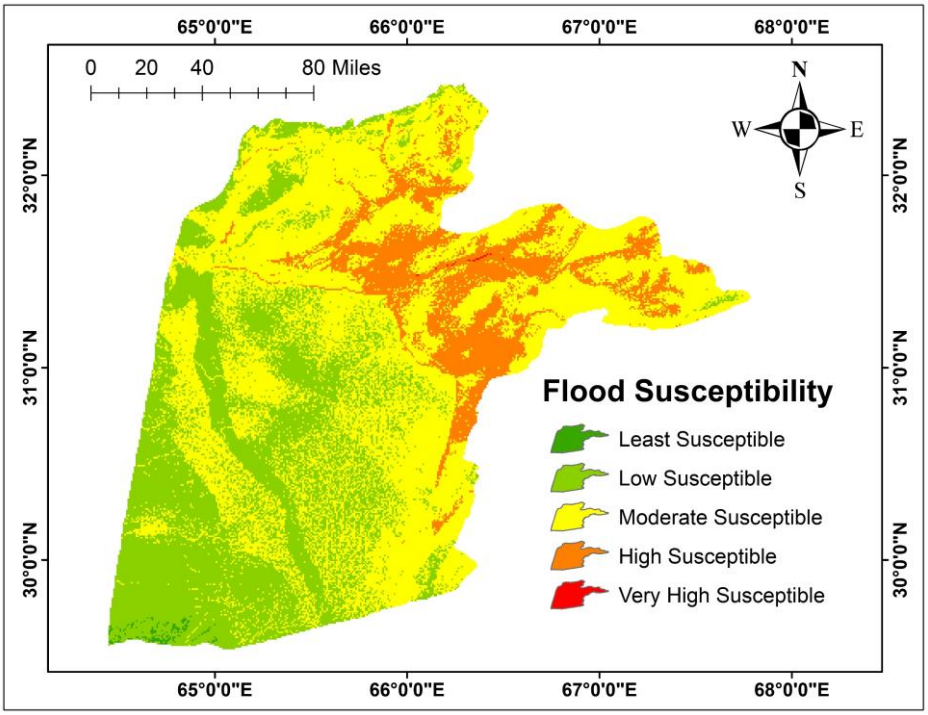

Figure 17 Flood Susceptibility Map of the Study Area

4 CONCLUSION

Due to its heavy and irregular rainfall patterns, the province of Kandahar in Afghanistan is particularly susceptible to flood dangers. Therefore, the study's aim was to map the flood susceptibility of Kandahar province, Afghanistan, and identify areas that are vulnerable to flooding. In order to identify and map the province's flood – prone areas, 11 flood causative factors (FCFs) such as runoff potential, slope, rainfall, flow accumulation, distance from rivers, topographic wetness index (TWI), drainage density, lithology, Digital elevation model (DEM), sediment transport index (STI), and curvature, were mapped, weighted, overlayed collectively, utilizing the integration of Geographic Information System (GIS), Multi – Criteria Decision – Making (MCDM), and Analytic Hierarchy Process (AHP).

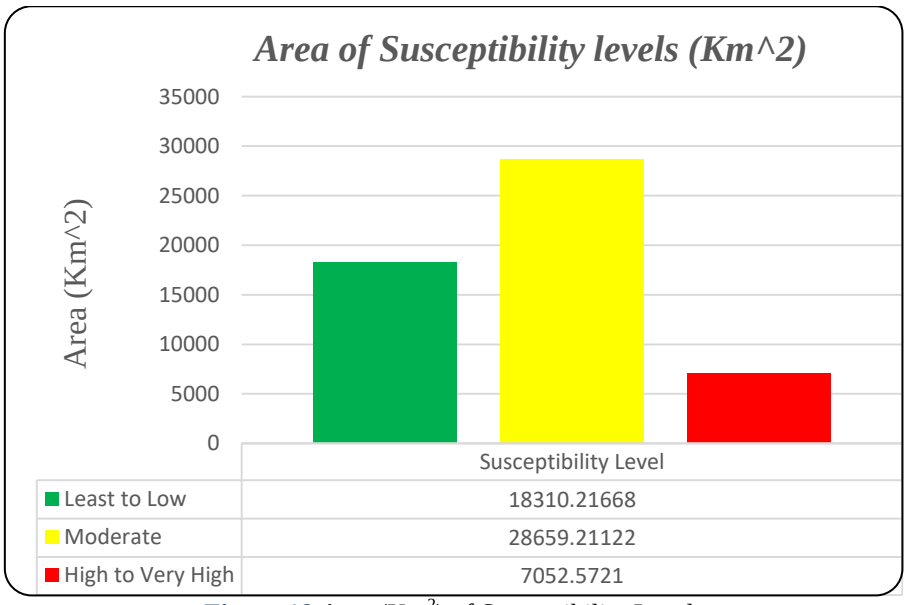

Figure 18 Area (Km^2) of Susceptibility Levels

Table 11 Area (%) and (Km^2) of Susceptibility Levels of All Districts of the Province

Districts	Area (Km^2)	Area (%) of susceptibility levels			Area (Km^2) of susceptibility levels		
		Least - low	Moderate	High - very high	Least - low	Moderate	High - very high
City	630	–	50.70	49.30	–	319.41	310.59
Arghistan	3668	–	57.13	42.87	–	2095.53	1572.47
Spin Boldak	5903	8.36	56.15	35.49	493.49	3314.53	2094.98
Arghandab	548	3.22	70.87	25.91	17.64	388.37	141.99
Maruf	3705	1.55	73.60	24.85	57.43	2726.88	920.69
Daman	4416	28.80	49.80	21.40	1271.81	2199.17	945.02
Shah Wali kot	3672	7.65	71.34	21.01	280.91	2619.60	771.49
Shorabak	4378	16.43	81.20	2.37	719.30	3554.94	103.76
Panjwayi	6821	43.88	54.08	2.04	2993.05	3688.80	139.15
Maywand	2850	38.46	60.13	1.41	1096.11	1713.71	40.18
Ghorak	1434	35.67	63.06	1.27	511.51	904.28	18.21
Khakrez	1252	14.08	84.94	0.98	176.28	1063.45	12.27
Reg	14745	72.32	27.68	–	10663.58	4081.42	–

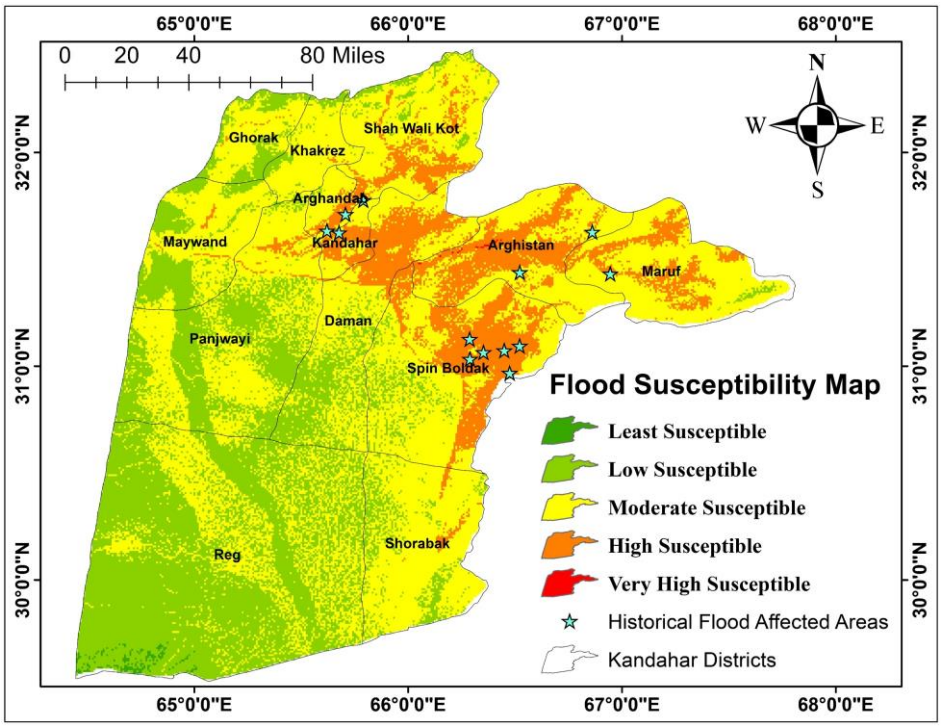

Figure 19 Validation of the Results

According to the results, the province's susceptibility to flooding is distributed as follows: in the term of area (Km^2), 18310.22Km^2 is least to low susceptible to flooding, 28659.21Km^2 is moderately susceptible to flooding, and 7052.57Km^2 is high to very high susceptible to flooding. And results indicated that 33.894%, 53.051%, and 13.055% of the province's areas have least to low, moderate, and high to very high susceptibility to flooding, respectively. According to the final flood susceptibility map, the majority of the high to very high susceptibility is found in the areas Kandahar city includes its surrounding, Arghistan district, Spin Boldak district, Arghandab district, Maruf district, Daman district, and Shah Wali Kot district. The study's flood susceptibility map, compared to historical flood event locations, shows greater accuracy, with most locations falling within high to very high flood susceptibility classes. According to the final flood susceptibility map, 13.055%, or 7052.57Km2, of the study's area total land area in Kandahar province is high to very high susceptible to flooding. To reduce flood vulnerability, government authorities must give these areas significant attention.

COMPETING INTERESTS

The authors have no relevant financial or non-financial interests to disclose.

FUNDING

For this work, the authors did not get any specific funding.

REFERENCES

[1] Balasubramanian, A. Floods as Natural Hazards. Presentation in August. 2005. DOI: https://doi.org/10.13140/RG.2.2.18898.96962.

[2] Duan, Y, Xiong J N, Cheng W M, et al. Increasing Global Flood Risk in 2005 – 2020 from a Multi – Scale Perspective. Journal of Remote Sensing. 2022, 14(21),5551. DOI: https://doi.org/10.3390/rs14215551.

[3] Njock, P G A, Shen S L, Zhou A N, et al. Evaluation of soil liquefaction using AI technology incorporating a coupled ENN/t–SNE model. Journal of Soil Dynamic and Earthquake Engineering, 2020, 130: 105988. DOI: https://doi.org/10.1016/j.soildyn.2019.105988.

[4] Jongman, B, Kreibich, H, Apel, H, et al. Comparative flood damage model assessment: towards a European approach. Natural Hazards and Earth System Sciences, 2012, 12(12): 3733-3752. DOI: https://doi.org/10.5194/nhess-12-3733-2012.

[5] Zang Q, Li J F, Singh, V P, et al. Spatio–temporal relations between temperature and precipitation regimes: Implications for temperature–induced changes in the hydrological cycle. Journal of Global and Planetary Change, 2013, 111: 57-76. DOI: https://doi.org/10.1016/j.gloplacha.2013.08.012.

[6] Rentschler, J, Salhab M, Jafino, B A, et al. Flood exposure and poverty in 188 countries. Nature Communications. 2022. https://doi.org/10.1038/s41467-022-30727-4.

[7] Hirabayashi, Y, Mahendran, R, Koirala, S, et al. Global flood risk under climate change. Journal of Nature Climate Chang, 2013, 3(9): 816-821. DOI: https://doi.org/10.1038/nclimate1911.

[8] Chris Courtne. The Nature of Disaster in China: The 1931 Yangzi River Flood. East Asian Science Technology and Medicine, 2021, 53(1-2): 106-110. DOI: https://doi.org/10.1163/26669323-53010004.

[9] Hooke, J, Mant, J. Geomorphological impacts of a flood event on ephemeral channels in SE Spain. Journal of Geomorphology, 2000, 34(3-4): 163-180. DOI: https://doi.org/10.1016/S0169-555X(00)00005-2.

[10] Maillet, G M, Vella C, Berne, S, et al. Morphological changes and sedimentary processes induced by the December 2003 flood event at the present mouth of the Grand Rhane River (Southern France). Marine Geology. 234, 2006, (1-4): 159-177. DOI: https://doi.org/10.1016/j.margo.2006.09.025.

[11] LIasat, M, del, C, Rigo, T, et al. The "Montserrat-2000" flash-flood event: a comparison with the flood that have occurred in the Northeastern Iberian Peninsula since the 14th Century. International Journal of Climatology, 2003, 23(4): 453-469. DOI: https://doi.org/10.1002/joc.888.

[12] The United Nation Office. Flash floods in southern Afghanistan kill at least 20. 2 March 2019. https://WWW.thenews.com.pk/latest/438842–at–least–20–killed–by–flash–floods–in–southern–afghanistan.

[13] AFP. Afghan search operations continue as flash floods kill more than 160. 27 Aug 2020. https://afghanistan.asia–news.com/en–GB/articles/cnmi_st/features/2020/08/27/feature–02.

[14] Afghan Red Crescent. Heavy Floods Have Damaged Spin Boldak of Kandahar Province, Southern Afghanistan. 1 Aug 2022. https://reliefweb.int/report/afghanistan/heavy–floods–have–damaged–many–lands–gardans–farms–and–houses–spin–boldak–district–kandahar–province–southern–afghanistan.

[15] Kuwait News Agency. Floods in Afghanistan and Pakistan. 23 April 2024. https://www.aljazeera.com/amp/news/2024/4/14/dozens–killed–in–afghanistan–as–heavy–rains–set–off–flash–floods.

[16] OCHA, Floods hit Eastern and Northeastern Afghanistan, 17 July 2024. https://reliefweb.int/disaster/fl–2024–000038–afg.

[17] Kaya, C M, Derin, L. Parameters and methods used in flood susceptibility mapping: a review. Journal of Water & Climate Change, 2024, 14(6): 1935-1960. DOI: https://doi.org/10.2166/wcc.2023.035.

[18] Dai, F C, Lee, C F. Landslide characteristics and slope instability modeling using GIS, Lantau Island, Hong Kong. Geomorphology, 2002, 42: 213-228. DOI: https://doi.org/10.1016/S0169-555X(01)00087-3.

[19] Kabalcı, E. Flexible Calculation Method–I. 2022. https://ekblc.files.workpress.com/2013/09/esnekhesaplamaya–giric59.pdf

[20] Zadeh, L A. Fuzzy logic: issues, contentions and perspectives, Proceedings of ICASS'94. IEEE International Conference on Acoustics and Signal Processing, Adelaide, SA, Australia 1994, 6, V1-183. DOI: https://doi.org/10.1145/197530.197667.

[21] Buckley, J J. Hayashi, Y. Fuzzy neural networks. A survey. Fuzzy Sets and Systems, 1994, 66: 1-13. DOI: https://doi.org/10.1016/0165-0114(94)90297-6.

[22] Malczewski, J. GIS and Multicriteria Decision Analysis. John Wiley & Sons, New York, 1999.

[23] Hong, H, Panahi, M, Shirzadi, A, et al. Flood susceptibility assessment in Hengfeng area coupling adaptive neuro-fuzzy inference system with genetic algorithm and differential evolution. Sci Total Environ, 2018, 621: 1124-1141. DOI: https://doi.org/10.1016/j.scitotenv.2017.10.114.

[24] Ajibade, F O, Ajibade, T F, Idowu, T E, et al. Flood-prone area mapping using GIS-based analytical hierarchy frameworks for Ibadan city, Nigeria. Journal of Multi-Criteria Decision-Analysis, 2021, 28(5-6): 283-295. DOI: https://doi.org/10.1002/mcda.1759.

[25] Shreve R L. Statical law of stream numbers. The Journal of Geology, 1966, 74(1): 17-37. DOI: https://doi.org/10.1086/627137.

[26] Strahler A N. Quantitative analysis of watershed geomorphology. Transactions, American Geophysical Union, 1957, 38(6): 913-920. DOI: https://dx.doi.org/10.1029/TR038i006p00913.

[27] Horton, R E. Drainage-basin characteristics. Trans Am Geophys Union, 1932, 13(1): 350-361. DOI: https://doi.org/10. 1029/TR013i001p00350.

[28] Youssef, A M, Pradhan, B, Hassan, A M. Flash flood risk estimation along the St. Katherine road, southern Sinai, Egypt using GIS based morphometry and satellite imagery. Environmental Earth Sciences, 2011, 62(3): 611-623. DOI: https://doi.org/10.3390/w11020364.

[29] Astutik, S, Pangastuti, E I, Nurdin, E A, et al. Assessment of Flood Hazard Mapping Based on Analytical Hierarchy Process (AHP) and GIS: Application in Kencong District, Jember Regency, Indonesia. Geosfera Indonesia, 2021, 6(3): 353. DOI: https://doi.org/10.19184/geosi.v6i3.21668.

[30] Hammami, S, Zouhri, L, Souissi, D, et al. Application of the GIS based multi-criteria decision analysis and analytical hierarchy process (AHP) in the flood susceptibility mapping (Tunisia). Arabian Journal of Geosciences. 2019, 12(21): 1-16. DOI: https://doi.org/10.1007/s12517-019-4754-9.

[31] Negese, A, Worku, D., Shitaye, A, et al. Potential flood-prone area identification and mapping using GIS-based multi-criteria decision-making and analytical hierarchy process in Dega Damot district, northwestern Ethiopia. Applied Water Science, 2022, 12, 255. DOI: https://doi.org/10.1007/s13201-022-01772-7.

[32] Allafta, H, Opp, C. GIS-based multi-criteria analysis for flood prone areas mapping in the trans-boundary Shatt Al-Arab basin, Iraq-Iran. Geomat Nat Haz Risk. 2021, 12(1): 2087-2116. DOI: https://doi.org/10.1080/19475705.2021.1955755.

[33] USDA-SCS. Soil survey of travis county texas agricultural experiment station. USDA soil conservation service, Washington, 1974.

[34] Zeng Z, Tang G Q, Hong Y, et al. Developmwnt of an NRCS curve number global dataset using the latest geospatial remote sensing data for worldwide hydrological applications. Remote Sensing Letters, 2017, 8(6): 528-536. https://dx.doi.org/10.1080/2150704X.2017.1297544.

[35] Khosravi, K, Pham, B T, Chapi, K, et al. A comparative assessment of decision trees algorithms for flash flood susceptibility modeling at Haraz watershed, northern Iran. Science of The Total Environment, 2018, 627: 744-755. DOI: https://doi.org/10.1016/j.scitotenv.2018.01.266.

[36] U.S Environmental Protection Agency. Soil Runoff Potential. Indicator Reference Sheet – March 6, 2022. https://WWW.epa.gov/system/files/documents/2022–3/soil–runoff–potential–indicator–reference–sheet–20220306.pdf

[37] Lee, S, Rezaie, F. Data used for GIS-based flood susceptibility mapping. Data Geol Ecol Oceanogr Space Sci Polar Sci, 2022, 41: 1-15. DOI: https://doi.org/10.22761/DJ2022.4.1.001.

[38] Das, S, Gupta, A. Multi-criteria decision based geospatial mapping of flood susceptibility and temporal hydro-geomorphic changes in the Subarnarekha basin, India. Geosci Front, 2021, 12(5): 101206. DOI: https://doi.org/10.1016/j.gsf.2021.101206.

[39] Mitra, R, Das, J. A comparative assessment of flood susceptibility modelling of GIS – based TOPSIS, VIKOR, and EDAS techniques in the sub–Himalayan foothills region of Eastern India. Environmental Science and Pollution Research, 2023, 30: 16036-16067. DOI: https://doi.org/10.1007/s11356–022–23168–5.

[40] Kron, W. Flood Risk = Hazard • Values • Vulnerability. Water International, 2005, 30(1): 58-68. DOI: https://doi.org/10.1080/02508060508691837.

[41] Elkhrachy, I. Flash flood hazard mapping using satellite images and GIS tools: a case study of Najran City, Kingdom of Saudi Arabia (KSA). The Egyptian Journal of Remote Sensing and Space Science, 2015, 18 (2): 261-278. DOI: https://doi.org/10.1016/j.ejrs.2015.06.007.

[42] Mahmoud, S H, Gan, T Y. Multi-criteria approach to develop flood susceptibility maps in arid regions of Middle East. J Clean Prod, 2018, 196: 216-229. DOI: https://doi.org/10.1016/j.jclepro.2018.06.047.

[43] Islam, M M, Sado, K. Development of flood hazard maps of Bangladesh using NOAA-AVHRR images with GIS. Hydrological Sciences Journal, 2000, 45(3): 337-355. DOI: https://doi.org/10.1080/02626660009492334.

[44] Bui, D T, Tsangaratos, P, Ngo, P T T, et al. Flash flood susceptibility modeling using an optimized fuzzy rule based feature selection technique and tree based ensemble methods. Science of The Total Environment, 2019, 668: 1038-1054. DOI: https://doi.org/10.1016/j.scitotenv.2019.02.422.

[45] Mirzaei, S, Vafakhah, M, Pradhan, B, et al. Flood susceptibility assessment using extreme gradient boosting (EGB), Iran. Earth Science Informatics, 2021, 14(1): 51-67. DOI: https://doi.org/10.1007/s12145-020-00530-0.

[46] Pradhan, B. Remote sensing and GIS-based landslide hazard analysis and cross-validation using multivariate logistic regression model on three test areas in Malaysia. Advances in Space Research, 2010, 45(10): 1244-1256. DOI: https://doi.org/10.1016/j.asr.2010.01.006.

[47] Tehrany, M S, Pradhan, B, Jebur, M N. Flood susceptibility analysis and its verification using a novel ensemble support vector machine and frequency ratio method. Stochastic Environmental Research and Risk Assessment, 2015a, 29(4): 1149-1165. DOI: https://doi.org/10. 1007/s00477-015-1021-9.

[48] Tehrany, M S, Pradhan, B, Mansor, S, et al. Flood susceptibility assessment using GIS-based support vector machine model with different kernel types. Catena, 2015b, 125: 91-101. DOI: https://doi.org/10.1016/j.catena.2014.10.017.

[49] Tehrany, M S, Lee, M J, Pradhan, B, et al. Flood susceptibility mapping using integrated bivariate and multivariate statistical models. Environmental Earth Sciences, 2014b, 72(10): 4001-4015. DOI: https://doi.org/10.1007/s12665-014-3289-3.

[50] Arslankaya, D, Göraltay, K. Çok Kriterli Karar Verme Yöntemlerinde Güncel Yaklası mlar (Current Approaches in Multi-Criteria Decision-Making Methods). Iksad Publications, Ankara, 2019.

[51] Saaty T L. The analytic hierarchy process planning, priority setting, resource allocation. McGraw Hill, New York, 1980. https://WWW.worldcat.org/research?qt=worldcat_org_all&q=0070543712.

[52] Mardani A, Jusoh A, Nor K M, et al. Multiple criteria decision-making techniques and their applications-a review of the literature from 2000 to 2014. Economic Research-Ekonomska Istrazivanja, 2015, 28(1): 516-571. DOI: https://dx.doi.org/10.1080/1331677X.2015.1075139.

[53] Marinoni O. Implementation of the analytic hierarchy process with VBA in ArcGIS. Computers and Geosciences, 2004, 30(6): 637-646. DOI: https://dx.doi.org/j.cageo.2004.03.010.

[54] Saaty T L, Vargas L G. Prediction, projection and forecasting. Kluwer Academic Publishers, Dordrecht. 1991. DOI: https://dx.doi.org/10.1007/978–94–015–7952–0.